Hindawi
Journal of Nanomaterials
Volume 2018, Article ID 1980357, 7 pages
https://doi.org/10.1155/2018/1980357

Research Article

Rapid Fabrication of Photoluminescent Electrospun Nanofibers without the Need of Chemical Polymeric Backbone Modifications

Mushtaq A. Sobhan,[1] Andrei Lebedev,[1] Leng L. Chng,[2] and Franklin Anariba[3]

[1]*Entropic Interface group, Engineering Product Development, Singapore University of Technology and Design, 8 Somapah Road, Singapore 487372*
[2]*Institute of Bioengineering and Nanotechnology, 31 Biopolis Way, The Nanos, Singapore 138669*
[3]*Surface and Materials Group, Engineering Product Development, Singapore University of Technology and Design, 8 Somapah Road, Singapore 487372*

Correspondence should be addressed to Franklin Anariba; franklin_anariba@sutd.edu.sg

Received 22 November 2017; Revised 29 March 2018; Accepted 19 August 2018; Published 31 October 2018

Academic Editor: Nader Shehata

Photoluminescent electrospun nanofibers were fabricated by incorporating a cyclopentadiene derivative AIE-active luminogen within the polymeric matrices of polyvinylpyrrolidone (PVP), poly(vinylidene fluoride)-co-hexafluoropropylene (PVDF-HFP), and poly(methylacrylate) (PMMA) under different solvents. Raman, infrared, and fluorescence spectroscopy showed the molecular integrity of the AIEgen is maintained during the electrospinning process while exhibiting a strong and uniformed phosphorescent radiative pathway of $\tau_{average} = 8.9\,\mu s$. This method allows for the rapid fabrication of photoluminescent nanofibers into a wide range of polymeric matrices without the need of chemical modifications. Taken together, the prepared electrospun phosphorescent nanofibers are a stepping stone for AIEgens to be applied in the digital manufacturing and design of smart textiles.

1. Introduction

Luminogens have gained tremendous interest because of their applicability in the fabrication of solid state emitters, such as organic light emitting diodes (OLED), required in display applications. However, traditional luminogens suffer from aggregation-induced quenching (AIQ) in the solid state form, mostly due to the formation of excimers and exciplexes species. Consequently, traditional luminogens have found limited applications in display devices because of its low dispersed concentration in films, providing inherently weak signals. In order to overcome this challenge, one strategy has been to chemically tailor luminogenic pendants to the backbone of polymers, refining polymeric architectures and granting optical capabilities, independent of conjugation as is the case in radical polymers [1]. Another strategy has been to synthetically modify polymeric backbones with pendants exhibiting aggregation-induced emission (AIE) properties [2, 3].

Recently, the fabrication of optical and electronic polymeric materials has been achieved through the use of the electrospinning technique, mainly due to its low cost and maintenance, flexible parametric tuning, green chemistry (use of small amounts of solvent), and high throughput [4]. One approach for the preparation of optical polymeric materials has been to electrospin polymer blends [5], such as polyfluorene derivatives/poly(methyl) methacrylate (PMMA) and phenylene vinylene derivatives/PMMA, using a single solution spinneret for the purpose of reducing AIQ to enhance luminescence efficiency. Results show an improved luminescence yield in comparison to spin-casted thin films, attributed to uniformed distribution due to geometrical constraints during the electrospinning process [6, 7]. In another approach, polymeric materials have been

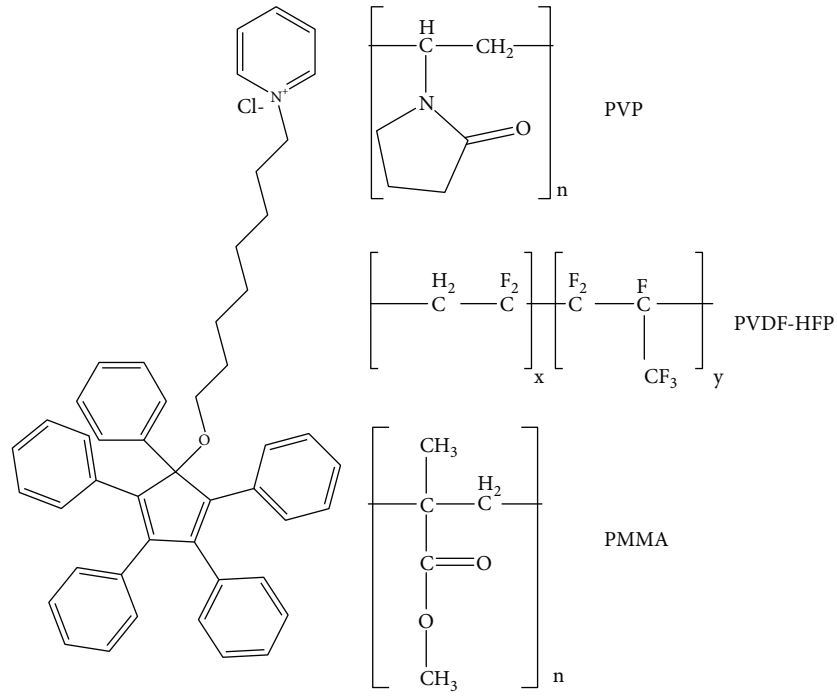

Figure 1: (a) Molecular structure of AIEgen 1-(1-(8-pyridiniumoctyloxy)-2, 3,4,5-tetraphenylcyclopenta-2,4-dienyl) benzene chloride (C8) displaying aggregation-induced emission (AIE) properties. For further information on C8 AIEgen, see reference [18]. (b) Molecular structure of polyvinylpyrrolidone (PVP), poly(vinylidene fluoride)-co-hexafluoropropylene (PVDF-HFP), and poly(methylacrylate) (PMMA).

synthetically modified with AIE-active pendants and subsequently electrospun [8, 9] into flexible solid state emitters [10], bacterial sensor [11], and for oil adsorption [12].

In a different approach, inorganic germanium nanocrystals have been incorporated into electrospun polymeric fibers, resulting in fiber webs with unique optical properties rivalling solution photoluminescence [13, 14]. Similarly, CdSe, CdS, and ZnS quantum dots (QD) have been incorporated into electrospun poly(9-vinylcarbazole) matrices to produce uniformed orange and red color solid state mat emitters with superior luminescence than thin films, reducing QD aggregation and its quenching effects. These mats were subsequently used along luminogen C545T [15] to fabricate white light OLEDs [15–17].

In this report, we undertake a different approach in the fabrication of photoluminescent electrospun polymeric nanofibers. An AIEgen [18] comprised of a cyclopentadiene head containing a pyridinium moiety as a tail, bridged by an 8-carbon alkane chain, is incorporated into polymeric matrices via electrospinning method. The AIEgen/polymer electrospun mat is subsequently characterized by various techniques. More specifically, we demonstrate that an AIEgen initially displaying low photoluminescence while dissolved in organic solvents can exhibit strong phosphorescence in an electrospun nanofiber when stimulated with UV light. This strategy eliminates the need to tether AIE-active pendants into polymeric backbones by chemical means, thus tremendously decreasing preparation time while minimizing potential solubility concerns.

1.1. Experimental. Figure 1(a) shows the molecular structure of the molecule displaying aggregation-induced emission (AIE) properties, 1-(1-(8-pyridiniumoctyloxy)-2,3,4,5-tetraphenylcyclopenta-2,4-dienyl) benzene chloride, hereafter referred to as **C8**, while Figure 1(b) exhibits the molecular structures of polyvinylpyrrolidone (PVP), poly(vinylidene fluoride)-co-hexafluoropropylene (PVDF-HFP), and poly(methylacrylate) (PMMA), the polymeric matrices used for electrospinning nanofibers.

1.1.1. Nanofiber Preparation. Polyvinylpyrrolidone (PVP), (MW: 130,000 Da), and ethanol (99.9% purity) were purchased from Sigma-Aldrich. The PVP solution was prepared by dissolving 0.3 g of PVP in 5 mL of ethanol and magnetic stirring for 1 h at room temperature. Subsequently, 4×10^{-3} g of **C8** molecules were added to the above solution and stirred for 30 min to reach a concentration of 1.23×10^{-3} M. Synthesis and solution-based photoluminescence studies of **C8** can be found in a previous work [18]. The resulting PVP/**C8** solution was loaded into a plastic syringe equipped with a 21 G needle. A high voltage of 20 kV was applied between the needle tip and the collector placed at a distance of 13 cm from the needle tip. The feeding rate for the solution was set at 0.6 mL/h through a syringe pump. The electrospun nanofibers were electrospun for 30 minutes and collected on a glass substrate or an aluminium foil to be subsequently dried in an oven at 60°C for 2 h. Similarly, 0.3 g of poly(vinylidene fluoride)-co-hexafluoropropylene (PVDF-HFP), (MW: 110,000 Da), were dissolved

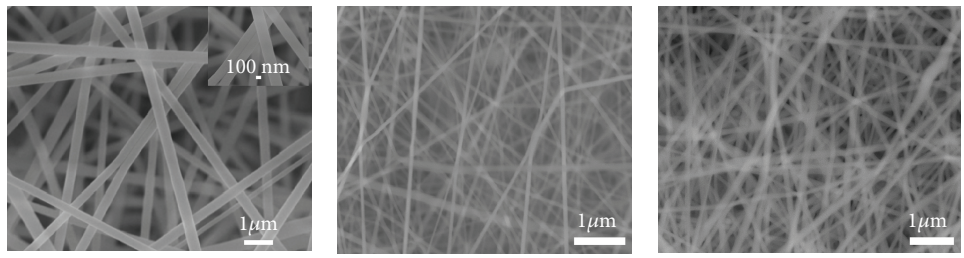

Figure 2: Scanning electron microscopy (SEM) images of electrospun (a) PVP/C8 nanofibers, (b) PVDF-HFP/C8 nanofibers, and (c) PMMA/C8 nanofibers.

in 5 mL dimethylformamide (DFM)/acetone (3.1 *v*/*v*) solution, followed by 30 min sonication and 30 min of magnetic stirring at room temperature. 0.3 g of poly(methylacrylate) (PMMA), (MW: 120,000 Da), were dissolved in 5 mL of dimethylformamide (DMF) solution, followed by magnetic stirring for 1 h. For both PVDF-HFP and PMMA solutions, 4×10^{-3} g of **C8** molecules were added to reach a concentration of 1.23×10^{-3} M, and the overall solutions were magnetically stirred for 30 min. All chemicals were research grade, commercially available, and were used as purchased. For PMMA, a high voltage of 15 kV was used between a needle tip and the substrate at a distance of 15 cm, at a flow rate of 0.8 mL/h. For PVDF-HFP, the voltage applied was 15 kV, set at a distance of 15 cm between the needle tip and the collector, at a flow rate of 1.0 mL/h.

1.1.2. Nanofiber Mat Characterization. The electrospun nanofibers deposited on glass substrates were freshly characterized and subsequently stored in a low humidity environment (dry cabinet at ~20% humidity). The morphology of the electrospun nanofiber mats was observed using a scanning electron microscopy (SEM, JEOL JSM-7600 F). The particle size analysis of the **C8** molecules in ethanol was obtained using a nanoparticle size analyser instrument (Nanosight NS300). Structural information of the electrospun nanofiber mats were gathered by Raman spectroscopy. Raman spectra were collected in a NT-MDT confocal Raman microscopic system with excitation laser wavelength of $\lambda_{ex} = 473$ nm, whereby the Si peak at 520 cm^{-1} was used as a reference for wavenumber calibration. UV-Vis molecular electronic absorption of the solutions and the UV-Vis reflection studies of the nanofiber mats were measured using a UV-Vis spectrophotometer (PerkinElmer). A UV light source equipped with white light, $\lambda_{ex} = 254$ nm, and $\lambda_{ex} = 365$ nm excitation wavelength and a UV lamp with an excitation wavelength of $\lambda_{ex} = 254$ nm and $\lambda_{ex} = 365$ nm were used to irradiate the nanofiber mats to subsequently digitally photograph their luminescence. Photoluminescence and lifetime of the nanofiber mats were measured using a fluorescence spectrometer (FSP920, Edinburgh Instruments, Livingston, U.K.). The fluorescence images were produced using a confocal microscope equipped with an excitation filter $\lambda_{ex} = 330$–380 nm and a barrier filter at $\lambda = 420$ nm (Nikon, UV-2A Filter). Digital photographs were taken with the camera of a Sony Experia Z3 handheld phone.

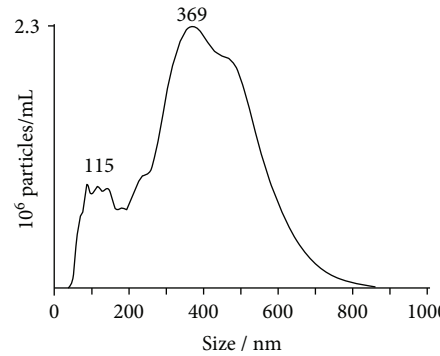

Figure 3: Nanoparticle tracking analysis of **C8** molecules in ethanol. The size distribution is bimodal and heterogeneous, ranging from ~50 to 800 nm.

2. Results and Discussion

The morphology of the electrospun nanofibers are shown in Figure 2. The nanofibers displayed a diameter range of 300 to 500 nm for PVP/C8 mats, 80 to 150 nm for PVDF-HFP/C8 mats, and 120–250 nm for PMMA/C8 mats. At the 30,000 times magnification level (see Figure 2(a) inset in upper right corner), the nanofibers showed smooth surfaces without the presence of beads or any other structural features associated with the electrospinning method or as previously reported for a HPS/PMMA blend [19].

The distribution and size of the **C8** aggregations within the PVP matrix could not be identified at this resolution, especially because **C8** molecules dissolved in ethanol displayed a heterogeneous size aggregation distribution ranging from ~50 to 800 nm with two noticeable peak at 115 and 369 nm, as shown in Figure 3. Although further studies are warranted to discern the nanoaggregation size and distribution within the electrospun nanofibers, nonetheless, the photoluminescent observed suggests the presence of nanoaggregations within the PVP matrix.

Raman spectroscopy provided invaluable information on the molecular structure of the electrospun nanofibers and molecular integrity of **C8** molecules within the matrix. Figure 4 shows Raman spectra in the range of 1400–1800 cm^{-1} for **C8** powder (a), PVP nanofiber mat (b), and PVP/**C8** nanofiber mat (c). **C8** molecules displayed strong

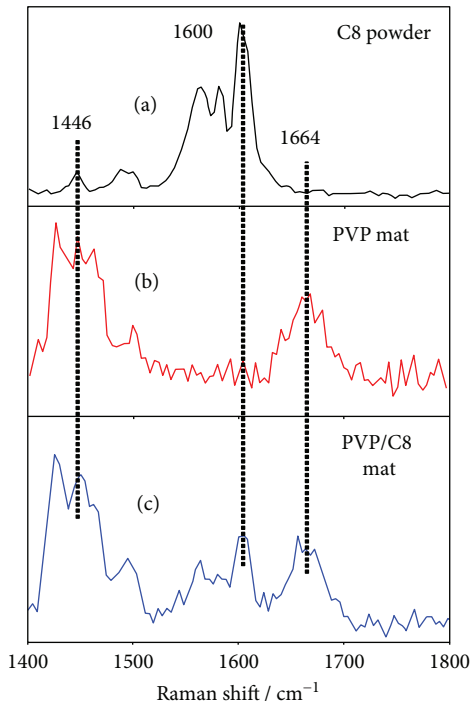

FIGURE 4: Raman spectra of (a) **C8** powder, (b) PVP nanofiber mat, and (c) PVP/**C8** nanofiber mat. The bands at 1600 cm^{-1}, which is assigned to ν(C=C) of **C8**, and at 1664 cm^{-1} associated with the carbonyl vibrations ν(C=O) of PVP, are clearly visible in the PVP/**C8** nanofiber mat spectrum.

Raman-active bands at 1600 cm^{-1}, 1580 cm^{-1}, and 1564 cm^{-1} and weak bands at 1500 cm^{-1} and 1446 cm^{-1}. The PVP nanofibers exhibited strong bands at 1664 cm^{-1}, 1462 cm^{-1}, 1446 cm^{-1}, 1426 cm^{-1} and a weak band at 1500 cm^{-1}. The PVP/**C8** nanofiber mats showed peaks at 1664 cm^{-1}, 1604 cm^{-1}, 1580 cm^{-1}, 1564 cm^{-1}, 1495 cm^{-1}, and 1450 cm^{-1}, representing bands associated with **C8** molecules and PVP. These results demonstrate that the molecular integrity of **C8** molecules was not affected by the electrospinning process and were instead embedded in nanoaggregate form within the PVP polymeric matrix. This is illustrated by the band at 1600 cm^{-1} associated with ν(C=C) [20] in **C8** molecules only, which is nonetheless observed in the PVP/**C8** electrospun nanofibers. Similarly, the peak at 1664 cm^{-1} assigned to ν(C=O) [21] in the PVP structure is also present in the PVP/**C8** nanofiber mats. In contrast, the band at 1446 cm^{-1}, which corresponds to a symmetric ring deformation [22], is observed in all three spectra since both PVP and **C8** molecules possess ring structures in their molecular structure.

The electronic absorption studies for solution and nanofiber mats are shown in Figure 5. Figures 5(a)–5(c) contrast UV-Vis absorbance spectra for **C8**, PVP, and PVP/**C8** ethanol solutions. AIE-active **C8** molecules with a concentration of 1.2×10^{-3} M showed a strong and broad absorption peak centered at 363 nm, which is an electronic π-π^* transition of the cyclopentadiene ring [23]. The strong absorption bands at $\lambda = 254$ nm and $\lambda = 272$ nm are associated with electronic π-π^* transitions of the pyridinium moiety [24]. Figure 5(b) corresponding to the PVP ethanol solution with a concentration of 4.6×10^{-4} M showed a featureless absorption throughout the spectral range, while the PVP/**C8** mixture resembles the spectrum of **C8** in ethanol solution in Figure 5(a). For the PVP/**C8** ethanol solution, the broad band at $\lambda = 363$ nm has been blue shifted to $\lambda = 358$ nm presumably by the presence of the electron donating ability of the nitrogen atom in the PVP structure. The band at $\lambda = 272$ nm lost intensity and was not discernible, but the peak at $\lambda = 254$ nm associated with **C8** molecules in the ethanol solution was observable.

Figures 5(d) and 5(e) depict the UV-Vis reflectance spectra of the PVP nanofiber and the PVP/**C8** nanofiber mats, respectively. In this case, the broad band at $\lambda = 365$ nm and the peaks at $\lambda = 254$ nm and $\lambda = 272$ nm associated with the **C8** molecules were clearly visible in the PVP/**C8** nanofiber mat spectrum but absent in the PVP nanofiber mat spectrum. The UV-Vis absorbance studies lend further support to the idea that **C8** molecules maintained molecular integrity and remained embedded within the PVP electrospun matrix.

The photoluminescent characteristics of the electrospun PVP/**C8** nanofiber mats are shown in Figure 6. Figure 6(a) reveals that the observed photoluminescent in the form of a broad band centered at $\lambda_{max} = 460$ nm is due to the embedded **C8** AIEgen within the polymeric matrix, presumably through nanoaggregations since PVP is nonphotoluminescent. Furthermore, the photoluminescent of PVP/**C8** nanofiber mats is highly uniformed, as shown in Figure 6(b), whereby fluorescence microscope images of the PVP and PVP/**C8** nanofiber mats are presented. The image mean intensity for the photoluminescent nanofiber mat was calculated to be 171.6 ± 4.4, while the PVP nanofiber mat image mean intensity was 0.01 ± 0.004, amounting to a coefficient of variance of 2.6% and 40% for the PVP/**C8** and PVP nanofiber mats, respectively, suggesting the surface of the PVP/**C8** electrospun nanofiber mats displays remarkably uniformed photoluminescent. These findings strongly indicate that the **C8** AIEgen is uniformly distributed in the PVP polymer matrix.

Figure 7 displays a lifetime photoluminescent curve for the embedded **C8** molecules. The time-resolved curve is best fitted with a double exponential decay, indicating the presence of two energy relaxation pathways for the excited molecules. A relatively fast relaxation time is shown in the upper inset with $\tau_1 = 5\,\mu$s (fraction of molecules $f_1 \cong 0.85$), while the slow relaxation time can be found in the lower inset with $\tau_2 = 31\,\mu$s ($f_2 \cong 0.15$). The weighted photoluminescent average was calculated to be $\tau_{average} = f_1\tau_1 + f_2\tau_2 = 8.9\,\mu$s, which falls in the range of a phosphorescent phenomenon associated with AIE-active molecules, indicating the fabrication process did not affect the emission lifetime. Photoluminescent lifetimes are related to radiative and nonradiative processes. It is not clear at this early stage the mechanism behind each of the two relaxation pathways; however, since the radiative lifetime is an intrinsic property of the luminogen, the nonradiative decay mechanism can be modified to become radiative by tailoring the polymer matrix/luminogen

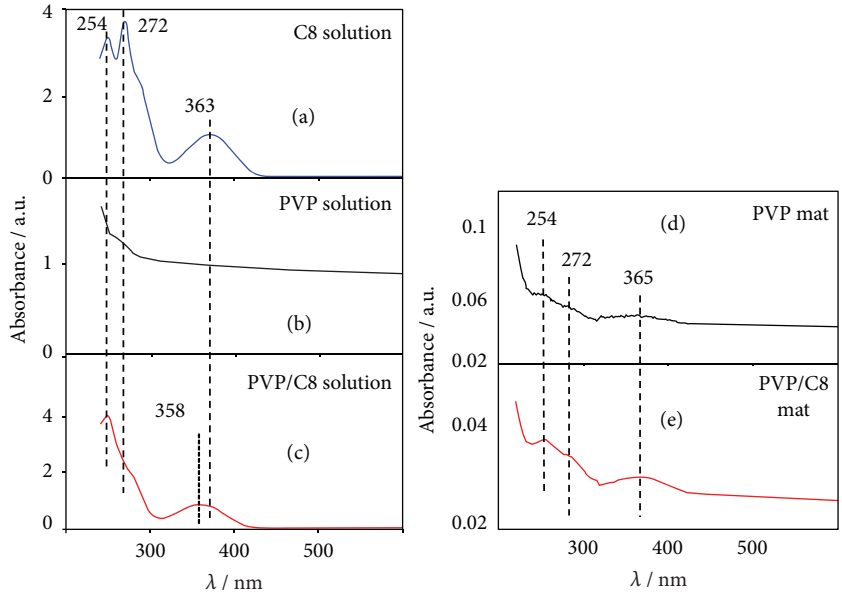

Figure 5: UV-Vis solution spectra of (a) **C8** ethanol solution, (b) PVP ethanol solution, and (c) PVP/**C8** ethanol solution. UV-Vis reflectance spectra of electrospun (d) PVP nanofiber mats, and (e) PVP/**C8** nanofibers mats.

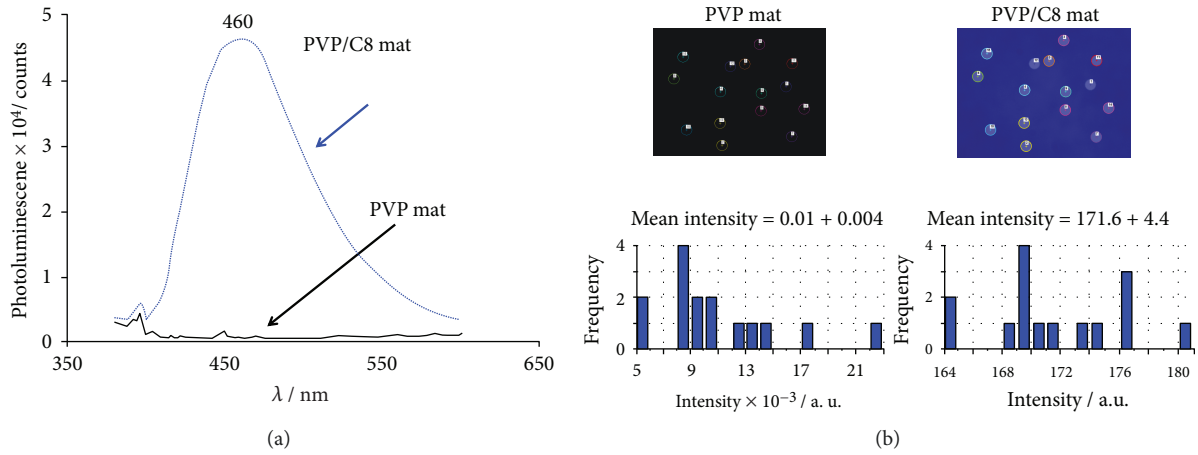

Figure 6: (a) Photoluminescent spectra of electrospun PVP and PVP/**C8** nanofiber mats with $\lambda_{ex} = 360$ nm. (b) Fluorescence microscope images and mean fluorescence intensity of (a) PVP nanofiber mats and (b) PVP/**C8** nanofiber mat. The mean intensity provided was probed randomly and its average and standard deviation corresponds to $n = 15$, visible as circles in the upper fluorescence images.

interaction, which within the AIE model means inhibiting the phenyl ring vibrational modes. We leave this analysis for a later manuscript.

The advantage of this fabrication method is the ability to incorporate AIEgens into a variety of solvents and polymeric matrices rather readily, obviating the need to tether AIE-active pendants into polymeric backbones by chemical means while minimizing solubility concerns. This improvement is demonstrated in Figure 8(a) where digital photographs of PVP and PVP/**C8** nanofiber mats under white light and UV irradiation are shown. The PVP nanofiber mats show no photoluminescent while the PVP/**C8** mats do exhibit a strong photoluminescence under both $\lambda_{ex} = 365$ nm and $\lambda_{ex} = 254$ nm excitation. Figure 8(b) shows digital photographs of electrospun nanofiber mats of poly(vinylidene fluoride)-co-hexafluoropropylene (PVDF-HFP)/**C8** (top panel) and poly(methylacrylate) (PMMA)/**C8** (bottom panel) displaying strong photoluminescence under $\lambda_{ex} = 365$ nm and $\lambda_{ex} = 254$ nm excitation. It is indeed quite a rapid and flexible photoluminescent nanofiber synthesis methodology.

3. Summary

We have demonstrated a successful and readily incorporation of an AIEgen within various polymeric matrices, such as PVP, PVDF-HFP, and PMMA, under various solvents to fabricate electrospun nanofiber mats (textiles) with smooth

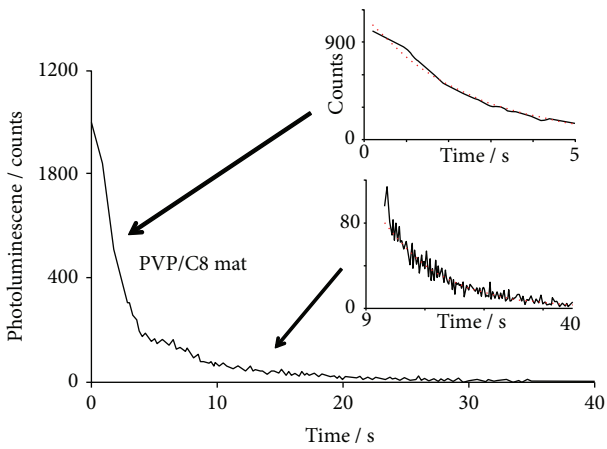

Figure 7: (a) Photoluminescent decay curve of the electrospun PVP/**C8** nanofiber mats. Upper inset is the exponential fit for the fast relaxation pathway (τ_1), while lower inset is the exponential fit for the slow relaxation pathway (τ_2).

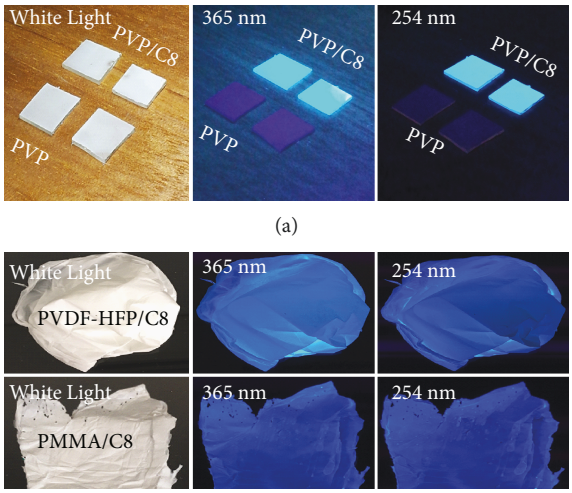

Figure 8: (a) Digital photographs of PVP and PVP/**C8** nanofiber mats on a glass substrate illuminated from above with white light, 365 nm and 254 nm excitation wavelength, respectively. (b) Digital photographs of PVDF-HFP/**C8** mats (top panel) and PMMA/**C8** mats (bottom panel) illuminated from above with white light but excited with 365 nm and 254 nm wavelength from below.

morphology without the need of chemical modification of the polymers and with minimal concerns in solubility. Both, the Raman and UV-Vis spectra, revealed that the AIEgen's molecular integrity remains intact within the polymeric electrospun nanofibers after electrospinning. The fluorescence emission spectrum indicated a strong and uniformed photoluminescence when excited with $\lambda_{ex} = 254$ nm and $\lambda_{ex} = 365$ nm, while the lifetime photoluminescence studies suggest the nanofibers follow a phosphorescent energy emission pathway. Taken together, the prepared electrospun phosphorescent nanofibers are a stepping stone for AIEgens to be applied in the digital manufacturing and design of smart textiles.

Conflicts of Interest

The authors declare no competing interests.

Acknowledgments

Associate Professor Wu Ping at SUTD and the MIT-SUTD International Design Centre (IDC) is acknowledged for instrument support. Leng L. Chng is supported by the Institute of Bioengineering and Nanotechnology (Biomedical Research Council, Agency for Science, Technology and Research, Singapore). PhD candidate Jeck Chuang Tan at EPD, SUTD, is gratefully acknowledged for helpful discussions on the subject.

References

[1] E. P. Tomlinson, M. E. Hay, and B. W. Boudouris, "Radical polymers and their application to organic electronic devices," *Macromolecules*, vol. 47, no. 18, pp. 6145–6158, 2014.

[2] B. Z. Tang, "Luminogenic polymers," *Macromolecular Chemistry and Physics*, vol. 210, no. 11, pp. 900–902, 2009.

[3] H. Wang, E. Zhao, J. W. Y. Lam, and B. Z. Tang, *Materials Today*, vol. 18, no. 7, pp. 365–377, 2015.

[4] S. RafieiA. Hamrang and D. Balkose, "Electrospinning process: a comprehensive review and update," in *Applied Methodologies in Polymer Research and Technology*, vol. 1, Apple Academic Press, 2014.

[5] J.-T. Wang, Y. C. Chiu, H. S. Sun et al., "Synthesis of multifunctional poly(1-pyrenemethyl methacrylate)-*b*-poly(*N*-isopropylacrylamide)-*b*-poly(*N*-methylolacrylamide)s and their electrospun nanofibers for metal ion sensory applications," *Polymer Chemistry*, vol. 6, no. 12, pp. 2327–2336, 2015.

[6] C.-C. Kuo, C.-H. Lin, and W. C. Chen, "Morphology and photophysical properties of light-emitting electrospun nanofibers prepared from poly(fluorene) derivative/PMMA blends," *Macromolecules*, vol. 40, no. 19, pp. 6959–6966, 2007.

[7] H. C. Chen, C.-L. Liu, C.-C. Bai, N.-H. Wang, C.-S. Tuan, and W.-C. Chen, "Morphology and photophysical properties of DB-PPV/PMMA luminescent electrospun fibers," *Macromolecular Chemistry and Physics*, vol. 210, no. 11, pp. 918–925, 2009.

[8] H.-J. Yen, C.-J. Chen, and G. S. Liou, *Chemical Communications*, vol. 49, no. 6, pp. 630–632, 2013.

[9] H.-J. Yen, J.-H. Wu, W.-C. Wang, and G.-S. Liou, "High-efficiency photoluminescence wholly aromatic triarylamine-based polyimide nanofiber with aggregation-induced emission enhancement," *Advanced Optical Materials*, vol. 1, no. 9, pp. 668–676, 2013.

[10] H.-J. Yen and G.-S. Liou, "Flexible electrofluorochromic devices with the highest contrast ratio based on aggregation-enhanced emission (AEE)-active cyanotriphenylamine-based polymers," *Chemical Communications*, vol. 49, no. 84, pp. 9797–9799, 2013.

[11] L. Zhao, Y. Chen, J. Yuan, M. Chen, H. Zhang, and X. Li, "Electrospun fibrous mats with conjugated tetraphenylethylene and mannose for sensitive turn-on fluorescent sensing of Escherichia coli," *ACS Applied Materials & Interfaces*, vol. 7, no. 9, pp. 5177–5186, 2015.

[12] W. Yuan, P.-Y. Gu, C.-J. Lu, K.-Q. Zhang, Q.-F. Xu, and J.-M. Lu, "Switchable fluorescent AIE-active nanoporous

fibers for cyclic oil adsorption," *RSC Advances*, vol. 4, no. 33, pp. 17255–17261, 2014.

[13] T. Abitbol, J. T. Wilson, and D. G. Gray, "Electrospinning of fluorescent fibers from CdSe/ZnS quantum dots in cellulose triacetate," *Journal of Applied Polymer Science*, vol. 119, no. 2, pp. 803–810, 2011.

[14] B. Ortac, F. Kayaci, H. A. Vural, A. E. Deniz, and T. Uyar, "Photoluminescent electrospun polymeric nanofibers incorporating germanium nanocrystals," *Reactive and Functional Polymers*, vol. 73, no. 9, pp. 1262–1267, 2013.

[15] Z. Liu, M. G. Helander, Z. Wang, and Z. Lu, "Efficient single-layer organic light-emitting diodes based on C545T-Alq_3 system," *The Journal of Physical Chemistry C*, vol. 114, no. 27, pp. 11931–11935, 2010.

[16] Y. Ner, J. . G. Grote, J. . A. Stuart, and G. . A. Sotzing, "White luminescence from multiple-dye-doped electrospun DNA nanofibers by fluorescence resonance energy transfer," *Angewandte Chemie International Edition*, vol. 48, no. 28, pp. 5134–5138, 2009.

[17] S.-Y. Min, J. Bang, J. Park et al., "Electrospun polymer/quantum dot composite fibers as down conversion phosphor layers for white light-emitting diodes," *RSC Advances*, vol. 4, no. 23, article 11585, 2014.

[18] F. Anariba, L. L. Chng, N. S. Abdullah, and F. E. H. Tay, "Syntheses, optical properties, and bioapplications of the aggregation-induced emission of 2,3,4,5-tetraphenylcyclopenta-2,4-dienyl benzene derivatives," *Journal of Materials Chemistry*, vol. 22, no. 36, p. 19303, 2012.

[19] L. Heng, X. Wang, Y. Dong et al., "Bio-inspired fabrication of lotus leaf like membranes as fluorescent sensing materials," *Chemistry – An Asian Journal*, vol. 3, no. 6, pp. 1041–1045, 2008.

[20] T. D. Klots, "Raman vapor spectrum and vibrational assignment for pyridine," *Spectrochimica Acta Part A: Molecular and Biomolecular Spectroscopy*, vol. 54, no. 10, pp. 1481–1498, 1998.

[21] D. L. A. de Faria, H. A. C. Gil, and A. A. A. de Queiróz, "The interaction between polyvinylpyrrolidone and I_2 as probed by Raman spectroscopy," *Journal of Molecular Structure*, vol. 478, no. 1-3, pp. 93–98, 1999.

[22] F. Anariba, U. Viswanathan, D. F. Bocian, and R. L. McCreery, "Determination of the structure and orientation of organic molecules tethered to flat graphitic carbon by ATR-FT-IR and Raman spectroscopy," *Analytical Chemistry*, vol. 78, no. 9, pp. 3104–3112, 2006.

[23] B. Z. Tang, X. Zhan, G. Yu, P. P. Sze Lee, Y. Liu, and D. Zhu, "Efficient blue emission from siloles," *Journal of Materials Chemistry*, vol. 11, no. 12, pp. 2974–2978, 2001.

[24] M. A. Pardo, J. M. Perez, M. A. del Valle, M. A. Godoy, and F. R. Diaz, "Pyridine based polymers: synthesis and characterization," *Journal of the Chilean Chemical Society*, vol. 59, no. 2, pp. 2464–2467, 2014.